

Removal

**Water Removal from Natural Gas by Adsorption: Modelling and Simulation
(FLUENT)**

Farah Liyana Bt Sahafea @ Shafie

7314

Dissertation submitted in partial fulfillment of
the requirements for the
Bachelor of Engineering (Hons)
(Chemical Engineering)

JULY 2009

University Teknologi PETRONAS

Bandar Seri Iskandar

31750 Tronoh

Perak Darul Ridzuan

CERTIFICATION OF APPROVAL

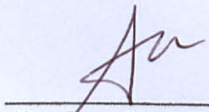
Water Removal from Natural Gas by Adsorption: Modelling and Simulation (FLUENT)

by

Farah Liyana Bt Sahafea @ Shafie

A project dissertation submitted to the
Chemical Engineering Programme
Universiti Teknologi PETRONAS
in partial fulfilment of the requirement for the
BACHELOR OF ENGINEERING (Hons)
(CHEMICAL ENGINEERING)

Approved by,



(Dr. Lau Kok Keong)

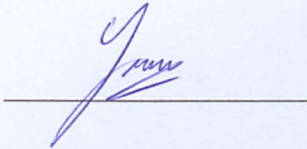
UNIVERSITI TEKNOLOGI PETRONAS

TRONOH, PERAK

July 2009

CERTIFICATION OF ORIGINALITY

This is to certify that I am responsible for the work submitted in this project, that the original work is my own except as specified in the references and acknowledgements, and that the original work contained herein have not been undertaken or done by unspecified sources or persons.

A handwritten signature in blue ink, appearing to read 'Farah Liyana Sahafea @ Shafie', is written over a horizontal line.

FARAH LIYANA SAHAFFEA @ SHAFIE

ABSTRACT

Water removal from natural gas is very important in order to prevent hydrates formation, corrosion in the pipeline and equipments and some of the industry need to meet specific water content within the product. The current and most commercial technology used nowadays is TEG Dehydrator but the weaknesses of this technology are regarding its size and much higher cost compared to other technology. Because of this, researches has been made to identify potential method and fortunately, now, one new technology that has been found to have high efficiency to remove water from natural gas is adsorption technology by molecular sieves Zeolite 3A. The main objective of this study is to confirm the effectiveness of adsorption method and its potential to overcome problems in TEG Dehydrator by performing the modeling and simulation of the whole process using FLUENT 6.3 Simulator. In using this software, the structure, geometry and grid of the pack-bed zeolite 3A adsorbent is modeled in Gambit and exported into Fluent for simulation and analysis. Before that, all parameters such as dimension of the bed, concentration and other important features should be identified first in order to obtain most accurate result for the simulation. The scope of study is basically focused on modeling and simulation of the adsorption process to get the most accurate result in order to prove the efficiency of this new method. The findings then will be evaluated whether it is proven or not that this new technology will be able to compete with current technology (TEG Dehydrator).

ACKNOWLEDGEMENT

First of all, I would like to thank Dr. Lau Kok Keong, my project supervisor, for guiding me in the duration of this project. I wouldn't have been able to complete this project without his great deal of assistance and support.

I would also like to thank the lecturers of Chemical Engineering Department of University Teknologi PETRONAS and others who attended my seminars, their suggestions and comments, during the project development, were very useful.

And also, thanks to Ms Salma, Postgraduate student which help in developing the UDF coding and thank to my family and friends for their moral support.

TABLE OF CONTENTS

Content	Page
Certification of Approval	II
Certification of Originality	III
Abstract	IV
Acknowledgement	V
Chapter 1: Introduction	1
1.1 Project Background	1
1.2 Problem Statement	2
1.3 Objective and Scope	4
1.4 Feasibility Study	4
Chapter 2: Literature Review and Theory	5
2.1 Literature Review Based on Books	5
2.2 Literature Review Based on Journals	8
2.3 Literature Review Based on Online Research	11
Chapter 3: Methodology	15
3.1 Research Methodology	15
3.2 Project Activities	16
3.3 Gantt Chart	17
3.4 Tools/Software	18
Chapter 4: Result and Discussion	20
4.1 Data Gathering/Data Analysis	20
4.2 UDF Code	21
4.3 Material and Condition for Simulation	21
4.4 Result Generated	
Chapter 5: Conclusion and Recommendation	30
5.1 Relevancy of Objectives	30

5.2 Suggested Future Work.	30
References	31
APPENDIX I	40
APPENDIX II	42

LIST OF TABLES

TABLE 4.1: Natural Gas Composition and Relevant Properties	7
TABLE 4.2: Physical Properties of Zeolite 3A	8
TABLE 4.3: Column Dimensions and Operating Conditions	22
TABLE 4.4: Pressure Drop	34

CHAPTER 1

INTRODUCTION

1.1 Project Background

In natural gas processing, one of the main step is to remove water content as efficient as possible before being exported or stored. The objective of this is to avoid formation of hydrates. Hydrates are referred as substances in crystal formed which result from physical combination of water and light hydrocarbon molecules. Hydrates can cause processing difficulty by disruption of process during natural gas treatment. Moreover, when there are accumulations of hydrates particles in orifice plates, valves and pipeline there are risks for blockage to occur because these hydrates particles tend to reduce the cross-sectional area of these equipments. Primary condition for hydrates to form in natural gas is the present of **water**. Water also can react with acid gases (CO_2 , H_2S) that cause corrosion to equipments and lines which then result in high cost of maintenance.

Throughout these years there are numbers of methods used in removing water which is Glycol Dehydration (TEG & DEG), Calcium Chloride (CaCl_2) Dehydration, Dry Desiccant Dehydrators using Molecular Sieves, Silica Gel, Activated Alumina or Activated Carbon, Membrane Systems, Ethylene Glycol (MEG) Injection and Methanol (MeOH) Injection. But the most commercial and widely used process is Triethylene Glycol (TEG) Dehydration.

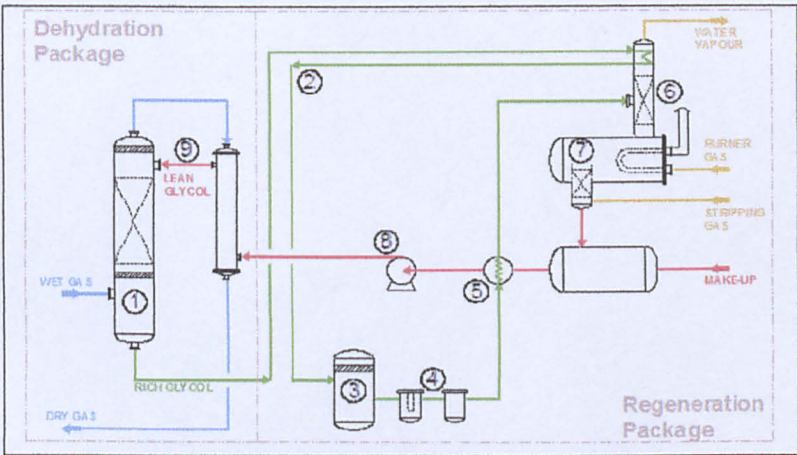


Figure 1.1: Schematic Flow of Triethylene Glycol (TEG) Dehydration.

In a typical TEG Dehydration package, the basic process is using counter current flow which occur when water saturated gas enters from the bottom of the contactor tower and flows upwards through the internal trays. Lean glycol enters the contactor tower near the top and cascades down through the contactor internals, making contact with the up-flowing gas stream. The counter-current flow and high contact surface area absorbs water into the glycol from the gas stream.

From there, dehydrated gas flows out of the top of the contactor, while the rich glycol flows out of the bottom of the contactor and to the glycol regeneration package. The TEG regeneration process typically involves passing the rich glycol through the still column to gain some heat before entering the flash drum. The glycol is then passed through particle filters to remove particulates and activated carbon filters to remove any dissolved hydrocarbon and/or chemical compounds. The rich glycol is heated in a cross exchanger to preheat the feed to the still column. Lean TEG (typically >99wt%) is then cooled and pumped back to the top of the contactor tower to repeat the process.

Until now, TEG Dehydration is referred as the most commercially used and most efficient in water removal application. But, there are also a few problems associate with this method. This is where the significant of this project takes account. Adsorption of water from natural gas using zeolite molecular sieves will be simulate and analyze whether the efficiency to adsorb water is compatible with TEG Dehydration and able to encounter problem faced by TEG Dehydration that will be stated in problem statement section.

1.2 Problem Statement

Although TEG Dehydration is labeled as first choice technology for water removal from natural gas industry, but there are still a few disadvantages of this method. Weakness of TEG Dehydration is in term of its equipment size, cost and thermal instability.

Equipment size

Equipment size

Since TEG Dehydrator is an absorption process, the size and dimension of the equipments is quite large because it is designed to hold an amount of liquid glycol. Moreover, it consists of two parts which is the dehydration section and regeneration section. This equipments required large space in the plant which is not very convenient for small plants.



Figure 1.2: Standard size of TEG Dehydrator

Cost

TEG also competes at a cost disadvantage with other glycols which is Diethylene Glycol (DEG), Monoethylene Glycol (MEG) and other technology. Consequently it is limited to those applications where its higher boiling point or lower volatility is valued.

Thermal instability.

During regeneration process, TEG had to be heated to about 204°C. But, due to TEG's thermal instability, it tends to undergoes slow degradation and polymerisation reactions. Corrosion products will build up in the TEG. Chlorides and sand can be entrained in the system with slugs of formation water.

The significant of this project is to find the most efficient method in water removal from natural gas process which comparable, effective and able to overcome disadvantage of current method.

1.3 Objective and Scope

The main objective of this project is to use adsorption process as an alternative to TEG Dehydration method in order to overcome the problems stated before. Zeolite 3A is identified as one of the adsorbent that has the potential to remove water from natural gas as efficient as TEG Dehydrator. Molecular Sieve Zeolite 3A is highly adsorbents which can be used in a wide range of industrial process including the drying of refrigerants, removal of water from ethene and olefinic hydrocarbons and petrochemical industry. The scope of the project is not an experimental research but based on the modeling and simulation using FLUENT 6.3 Software. By simulating the whole process in FLUENT, the efficiency of this method will be obtained and compare with the current process which is TEG Dehydrator. The result of pressure drop also will be validate with laboratory result.

1.4 Feasibility Study

The feasibility study of the project within the scope is to get the best way how to manage the entire task in completing the research project. For the first part of the research project, understanding of previous research done is made. All relevant information is gathered and become the guide and basis in completing this study. Simulation of the process is done later in order to observe the efficiency of this method by analyzing the pressure drop across the adsorption bed.

CHAPTER 2 LITERATURE REVIEW

Water adsorption by zeolite from natural gas is applying the method of adsorption process where Zeolite 3A molecular sieves is arrange in a pack-bed column so that natural gas will flow from the bottom, passed through it, and leave from the top as dehydrated gas. Water vapor will be adsorbed on the surface of the zeolite particle and a separation of water from natural gas is accomplished. When the bed is almost saturated, the flow on this bed is stop and the bed is regenerated. Regeneration Zeolite 3A can be reactivated by thermal sewing, vacuum desorption or gas displacement, the regeneration mode is based on the feed composition.

2.1 Literature Review Based on Books

2.1.1 Adsorption Engineering (By Motoyuki Suzuki)

Adsorption equilibrium

When an adsorbent is in contact with the surrounding fluid of a certain composition, adsorption takes place and after a sufficiently long time, the adsorbent and the surrounding fluid reach equilibrium. In this state, the amount of the component adsorbed on the surface mainly of the micropore of the adsorbent is determined. The relation between amount adsorbed, q and concentration in the fluid phase, C at temperature, T is called the adsorption isotherm at T .

$$q = q(C) \text{ at } T$$

Adsorption isotherms can be differentiated into two which is the surface adsorption and micropore adsorption.

- Surface adsorption

The simplest model of adsorption on a surface is that in which localized adsorption takes place on an energetically uniform surface without any interaction between adsorbed molecules. When surface coverage or fractional filling of the micropore is $\theta(q/q_0)$ and the concentration in the fluid, $C(p/RT)$, the adsorption rate is expressed as $k_a p(1-\theta)$

assuming first order kinetics with desorption rate given as $k_d\theta$. Then equilibration of adsorption rate and desorption rate gives the equilibrium relation as

$$\theta = Kp / (1 + Kp) \text{ (Langmuir isotherm)}$$

K is k_a/k_d called as equilibrium constant.

- Micropore adsorption

In micropore of size comparable to the size of adsorbate molecule, adsorption take place by attractive force from the wall surrounding the micropore and the adsorbate molecules start to fill the micropore volumetrically. In this type of adsorption, the adsorption equilibrium relation for a given adsorbate-adsorbent combination can be expressed independent of temperature by using the adsorption potential.

$$W = q / \rho = W(A)$$

Where W is the volume of micropore filled by the adsorbate and ρ is the density of the adsorbed phase. Adsorption potential, A is defined as the difference in free energy between the adsorbed phase and the saturated liquid.

$$A = -RT \ln(p / p_s)$$

2.1.2 Adsorbents: Fundamentals and Applications (By Ralph T. Yang)

Regeneration

Adsorptive gas separation processes can be divided into two types which bulk separation and purification. The former involves adsorption of significant fraction, 10% by weight or more from a gas stream whereas in purification, <10% (usually <2%) by weight of a gas stream is adsorbed. For purification, temperature swing adsorption (TSA) is generally the process of choice. For bulk separation, pressure swing adsorption (PSA) is more suitable.

Temperature Swing Adsorption

In this process cycle, the bed is regenerated by raising the temperature. The most convenient way for raising the temperature is by purging the bed with preheated gas. Because heating is slow and often a rate-limiting step, the length of each cycle usually

ranges from several hours to over a day. In order to make the time length of the adsorption step comparable with that of regeneration, the cycle is used only for purification purpose.

2.1.3 Transport Processes and Separation Process Principles (By Christie John Geankoplis)

Equilibrium Relation for Adsorbents

The equilibrium between the concentration of a solute (in this project solute refers to water) in the fluid phase and its concentration on the solid resembles somewhat the equilibrium solubility of a gas in a liquid. Data are plotted as adsorption isotherms as shown in Figure I. The concentration in the solid phase (refer to zeolite 3A) is expressed as q , kg adsorbate/kg adsorbent and in the fluid phase as c , kg adsorbate/m³ fluid.

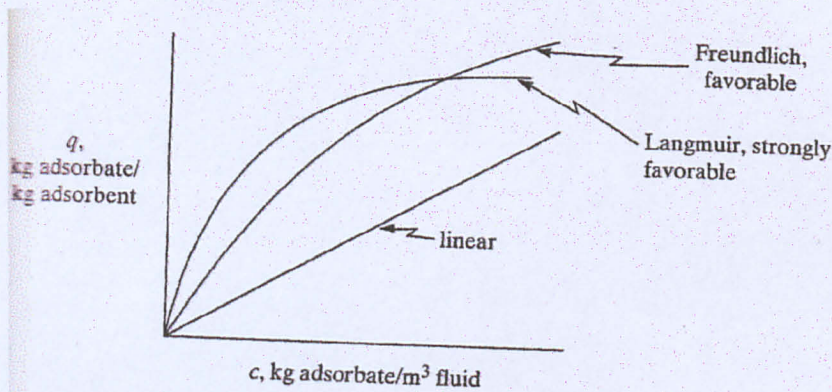


Figure 2.1: Common type of adsorption isotherms

$$Q = kc$$

Where k is constant determined experimentally, m³/kg adsorbent. This linear isotherm is not common, but in the dilute region it can be used to approximate data for many systems.

The Freundlich isotherm equation, which is empirical, often approximates data for many physical adsorption systems and is particularly useful for liquids:

$$Q = kc^n$$

Where k and n are constants and must be determined experimentally. If a log-log plot is made for q versus c , the slope is the dimensionless exponent n . The dimensions of k

depend on the value of n . This equation is sometimes used to correlate data for hydrocarbon gases on activated carbon.

The Langmuir isotherm has a theoretical basis and is given by the following, where q_0 and k are empirical constants:

$$Q = (q_0 c) / (k + c)$$

Where q_0 is kg of adsorbate/kg solid and k is kg/m^3 . The equation was derived assuming that there are only a fixed number of active sites available for adsorption, that only a monolayer is formed and that the adsorption is reversible and reaches an equilibrium condition. By plotting $1/q$ versus $1/c$, the slope is k/q_0 and the intercept is $1/q_0$. Almost all adsorption systems show that as the temperature is increased, the amount adsorbed by the adsorbent decreased strongly. This is useful since adsorption is normally at room temperatures and desorption can be attained by raising the temperature.

2.1.4 Gas Separation by Adsorption Processes (Ralph T. Yang)

RATE PROCESSES IN ADSORBERS

Adsorptive gas separation processes are carried out in fixed-bed adsorbers which contain porous adsorbent particles or pellets. Mathematical models are needed to understand the dynamics of adsorbers, thereby controlling and predicting the separation results [5].

Governing Equations for Absorbers

The mass balance within a spherical pellet is described by by:

$$D_e \left(\frac{\partial^2 C^p}{\partial r^2} + \frac{2}{r} \frac{\partial C^p}{\partial r} \right) = \frac{\partial q}{\partial t}$$

where D_e is the effective diffusivity C^p is the gas-phase concentration inside the pore, q is the amount adsorbed per volume of pellet. The factor 2 in $2/r$ is replaced by 1 for cylindrical and 0 for platelet pellets. In writing this equation the adsorbate accumulation in the gas phase, $\alpha \partial C^g / \partial t$ (where α is the void fraction within the pellet), has been neglected and would otherwise appear on the right hand side.

The mass balance for the bulk flow in the bed, or the interpellet phase, is:

$$-D_z \frac{\partial^2 C}{\partial z^2} + \frac{\partial uC}{\partial z} + \frac{\partial C}{\partial t} + \frac{1-\varepsilon}{\varepsilon} ka(C - C_R^p) = 0$$

where:

- D_z = axial dispersion coefficient
- u = interstitial velocity
- C = interpellet concentration
- ε = interpellet void fraction
- a = exterior surface area of pellets per volume of bed
- k = average mass transfer film coefficient
- C_R^p = concentration at the pellet surface (R_p = radius of pellet)
- t = time
- z = distance in the bed from the entrance

In this equation concentration is assumed to be uniform in the radial direction and radial dispersion coefficient is neglected.

Mass Transfer Film Coefficient

Much of mass transfer data in packed beds have been correlated by the Ranz-Marshall equation

$$Sh = 2.0 + 0.6Sc^{1/3} Re^{1/2}$$

where Sh , Sc , and Re stand for Sherwood, Schmidt, and Reynolds numbers, respectively.

A recent correlation of this type has been made by Wakao and Funazkri. Their correlation is significant because they pointed out an error made in most of the previous correlations. The resulting correlation for $3 < Re < 10^4$ is

$$Sh = 2.0 + 1.1Sc^{1/3} Re^{0.6}$$

R. Byron Bird et al. defines Sherwood, Schmidt and Reynolds numbers as:

$$Sh = \frac{k_x l_o}{D_{AB}}$$

$$Sc = \frac{\mu}{\rho D_{AB}}$$

$$Re = \frac{l_o v_o \rho}{\mu}$$

where k_x is mass transfer coefficient, l_o is characteristics length, D_{AB} is molecular diffusivity between components A and B, μ is dynamic viscosity, ρ is density, and v_o is velocity.

Axial Dispersion

If a concentration gradient exists in a packed bed, a diffusive mass flux will occur. In addition, eddy (turbulent) diffusion due to the flow also contributes to the mass flux. The resultant flux is referred to as *mass dispersion*, which may be expressed mathematically in terms of Fick's law, where the proportionality constant is called *dispersion coefficient*. Dispersion occurs in both radial and axial directions in the bed. The radial dispersion is, however, regarded as unimportant, when the adsorbed bed diameter is far greater than the particle diameter.

When axial dispersion is included in modeling fixed-bed adsorbers, equations given below should be used. It is important to bear in mind, however, that this equation was obtained by using an axial dispersion coefficient given by the following equation.

$$\frac{\varepsilon D_z}{D_m} = 20 + 0.5 Sc Re$$

Macropore Diffusion

In the Knudsen diffusion regime, the exchange of momentum from the gas molecules to the pore wall is important. The momentum given up p the colliding molecules to the wall

must be balanced by the force exerted on the two ends of the pore, which is given by the pressure gradient across the pore. The diffusivity is given by:

$$D_k = 9.7 \times 10^3 r_p \left(\frac{T}{M} \right)^{1/2}$$

where:

r_p	=	pore radius, cm
M	=	molecular weight
T	=	temperature, K
D_k	=	Knudsen diffusivity, cm ² /s

Note that this equation applies only when the mean free path is much greater than the pore radius. The value of D_k should not exceed molecular diffusivity.

The molecular diffusivity for a binary mixture gas can be evaluated by the familiar Chapman-Enskog equation:

$$D_m = 0.0018583 \frac{T^{3/2} (1/M_A + 1/M_B)^{1/2}}{P \sigma_{AB}^2 \Omega_{AB}}$$

where:

D_m	=	molecular diffusivity between A and B, cm ² /s
T	=	temperature, K
M_A & M_B	=	molecular weights
P	=	total pressure, atm
σ_{AB} , ϵ_{AB}	=	constants in the Lennard-Jones potential-energy function for the pair AB; σ_{AB} is in Å
Ω_{AB}	=	collision integral, a function of $k_B T / \epsilon_{AB}$ where k_B is Boltzmann's constant.

In adsorption and desorption processes, $N_A \approx -N_B$ (the negative sign indicates that the two fluxes are in opposite directions). Thus

$$D \approx \frac{l}{(l/D_m) + (l/D_k)}$$

This result was obtained earlier by Bosanquet [34], and Pollard and Present

The actual diffusion path will not equal the distance in the radial direction, but will be quite tortuous. The actual path depends on the pore structure. It is customary to define the ratio between the actual diffusion path length and the net distance in the direction of flux, or the radial distance, as *tortuosity factor*, τ . Taking into account that the volume occupied by the solid is not available for pore diffusion, the value of D for single pores can be converted to effective diffusivity:

$$D_e = \frac{\alpha D}{\tau}$$

where α is the intrapellet void fraction.

D. R. Lide [36] defines the tortuosity factor as

$$\tau = (2 - \alpha)^2 / \alpha$$

Micropore Diffusion

Micropore diffusion occurs in the pores of dimensions comparable to the diameter of the diffusing molecules. In micropore diffusion, the diffusing molecule never escapes the adsorbent force field. In such small pores, it is difficult to differentiate between the adsorbed molecules and the gaseous molecule in the central of the pore. It is preferable that the entire gas molecules within the microparticle are considered as the adsorbed phase.

In the microporous adsorption process, the adsorbent surface concentration is time dependent. The adsorbent diffusivity is usually determined from the so called *uptake*

curve. Uptake curve contains information of the adsorbed amount at specific time (M_t) to the adsorbed amount at equilibrium (M_e) and plot against time.

2.2 Literature Review Based on Journals

2.2.1 Adsorption of Water and Ethanol Vapors on 3A and 4A molecular sieves

(By Daniel Michael Leo)

Langmuir Isotherm Model

Adsorption isotherms provide the equilibrium relationship between the amount of substance adsorbed onto a zeolite surface at different concentrations and temperatures. One of the simplest means to describe the adsorption behavior is by Langmuir equation

$$q_i = q_i^s(T) \frac{K_i(T)P_i}{1 + K_i(T)P_i}$$

q_i = adsorption capacity of species i in mol/kg of zeolite

P_i = partial pressure of species i in Pascal.

q_i^s , K_i = Langmuir isotherm empirical constants (parameter) of species i which are obtained by non linear regression of actual experimental data.

Multiregional Extended Langmuir Isotherm Model

The multiregional extended Langmuir (MREL) isotherm model takes into account differences in selectivity of absorbable species. The MREL model assumes that there are two distinct sites or regions that absorbable species may adsorb on to. In the case of binary mixture, the MREL model assumes that one species adsorb upon both sites while the other species adsorb upon only one of the sites due to size exclusions. This model attains thermodynamic consistency due to the assumption that the adsorption capacities of both species are identical on the areas that both species bind to. The amount of water and ethanol adsorbed onto zeolite 4A can be expressed as

$$q_{w,4A} = q_e^s(T) \frac{K_w(T)P_w}{1 + K_e(T)P_e + K_w(T)P_w}$$

$$q_{e,4A} = q_w^s(T) \frac{K_e(T)P_e}{1 + K_e(T)P_e + K_w(T)P_w}$$

In turn, the amount of water and ethanol adsorbed on 3A sites might expressed as

$$q_{w,3A} = (q_w^s(T) - q_e^s(T)) \frac{K_w(T)P_w}{1 + K_w(T)P_w}$$

$$q_{e,3A} = 0$$

2.2.2 Microcalorimetric study of sorption of water and ethanol in zeolites 3A and 5A

(By E. Lalik, R. Mirek, J. Rakoczy, A. Groszek)

Sorption of water and ethanol in zeolites 3A and 5A was investigated using gas flow-through microcalorimetry in view of finding differences in these materials performance as potential sorbents in the process of drying of ethanol. In microcalorimetric experiments, both zeolites show comparable properties for the sorption of water, but they differ profoundly in their sorption of ethanol, which was negligible small in zeolite 3A compared to zeolite 5A, in spite of the much larger enthalpy of sorption of ethanol in zeolite 3A. The difference can be explained in terms of a steric hindrance preventing the ethanol molecules from entering the narrow pores of the 3A structure, with the 5A structure remaining easily accessible for both the water and ethanol molecules alike. The research proposes to use a size selectivity index, defined as the ratio of sorption capacity of water and ethanol, to characterize the applicability of a zeolite as sorbent for drying of ethanol. The thermal effect of sorption of water in zeolite 3A was found to be a function of the nature of carrier gas, He or N₂, used in microcalorimetric measurements.

2.2.3 Thermodynamic and Structural Features of Water Sorption in Zeolites

(By Marie Hellene Simonot-Grange)

The water adsorption capacity of zeolites is a function of pressure and temperature. Desorption of zeolites may be of three types, wherein the crystal lattice undergoes (1) no or little change, (2) a reversible change, or (3) an irreversible change. In the first two cases, the divariance of the zeolite-water vapor equilibrium results in networks of isobars, isotherms, and isosteres which can be transformed into a "characteristic" curve following the Polanyi-Dubinin theory. Because the volume of the micropores of a zeolite structure is constant, the isotherms and "characteristic" curve can

be transformed linearly. During desorption, if the volume of the micropores varies due to a change of structure, the curves show linearity breaks.

On the basis of X-ray diffraction, differential thermal and thermal gravimetric analyses, the equilibrium curves and structural changes of heulandite and stilbite were determined, using specially designed equipment. In the reversible adsorption range, heulandite shows no linearity breaks in the transforms and no structural variation. Stilbite, however, shows a linearity break in the transforms corresponding to a structural change.

2.2.4 Zeolite as Natural Gas Adsorbents.

A group of students from Chemical and Resources Engineering Department from Universiti Teknologi Malaysia has done their research on the potential of zeolite as adsorbent for natural gas. This research studies the adsorptive characteristics of various adsorbents such as zeolite A, X, Y, mordenite and ZSM-5 as well as mesoporous materials such as MCM-41 and SBA-15. The study was carried out on gases such as N_2 , CO_2 , and CH_4 . The result shows that zeolite is an excellent adsorbent for gas and the gas adsorption characteristics of gas molecules depend mainly on the accessibility of the molecules (pore size or pore opening) to the adsorption sites. In general, modifications can enhance the adsorption characteristics of zeolites. The study is based on adsorption of zeolite on gases but it is proven that zeolite is one of the excellent adsorbent and could be apply on water vapor adsorption.

2.3 Literature Review Based on Online Research (Internet)

2.3.1 Natural Gas

Since the project is focused on removing water from natural gas, it is essential to research on the natural gas composition and its properties. Natural gas, in itself, might be considered a very uninteresting gas because it is colorless, shapeless, and odorless in its pure form. Natural gas is combustible, and when burned it gives off a great deal of energy. Unlike other fossil fuels, however, natural gas is clean burning and emits lower levels of potentially harmful byproducts into the air. We require energy constantly, to

heat our homes, cook our food, and generate our electricity. It is this need for energy that has elevated natural gas to such a level of importance in our society, and in our lives.

Natural gas is a combustible mixture of hydrocarbon gases. While natural gas is formed primarily of methane, it can also include ethane, propane, butane and pentane. The composition of natural gas can vary widely, but figure below outlined the typical makeup of natural gas before it is refined.

Methane	CH ₄	70-90%
Ethane	C ₂ H ₆	
Propane	C ₃ H ₈	0-20%
Butane	C ₄ H ₁₀	
Carbon Dioxide	CO ₂	0-8%
Oxygen	O ₂	0-0.2%
Nitrogen	N ₂	0-5%
Hydrogen sulphide	H ₂ S	0-5%
Rare gases	A, He, Ne, Xe	trace

Figure 2.2: Typical Composition of Natural Gas

Within natural gas, the typical sulphur content is 5.5 mg/m³ and the water vapor content is less than 80 mg/m³, and is typically 16 to 32 mg/m³ which is very small amount but still have to be remove during natural gas processing since the occurrence of it may result in problems later.

Natural gas is mainly consist of methane. Methane is a molecule made up of one carbon atom and four hydrogen atoms, and is referred to as CH₄. Ethane, propane, and the other hydrocarbons commonly associated with natural gas have slightly different chemical formulas and occur in natural gas with much lower amount compared to methane. Natural gas is considered 'dry' when it is almost pure methane, having had most of the other commonly associated hydrocarbons removed. When other hydrocarbons are present, the natural gas is 'wet'.

2.3.2 Zeolite

Zeolites are microporous, aluminosilicate minerals commonly used as commercial absorbents. As of January 2008, 175 unique zeolite frameworks have been identified, and over 40 naturally occurring zeolite frameworks are known. Zeolites have a porous structure that can accommodate a wide variety of cations, such as Na^+ , K^+ , Ca^{2+} , Mg^{2+} and others. These positive ions are rather loosely held and can readily be exchanged for others in a contact solution. Some of the more common mineral zeolites are analcime, chabazite, clinoptilolite, heulandite, natrolite, phillipsite, and stilbite. An example mineral formula is: $\text{Na}_2\text{Al}_2\text{Si}_3\text{O}_{10}\cdot 2\text{H}_2\text{O}$, the formula for natrolite.



Figure 2.3: Zeolite

Natural zeolites form where volcanic rocks and ash layers react with alkaline groundwater. Zeolites also crystallize in post-depositional environments over periods ranging from thousands to millions of years in shallow marine basins. Naturally occurring zeolites are rarely pure and are contaminated to varying degrees by other minerals, metals, quartz, or other zeolites. For this reason, naturally occurring zeolites are excluded from many important commercial applications where uniformity and purity are essential.

Zeolites are the aluminosilicate members of the family of microporous solids known as "molecular sieves." The term molecular sieve refers to a particular property of these materials, i.e., the ability to selectively sort molecules based primarily on a size exclusion process. This is due to a very regular pore structure of molecular dimensions. The maximum size of the molecular or ionic species that can enter the pores of a zeolite is controlled by the dimensions of the channels. These are conventionally defined by the ring size of the aperture, where, for example, the term "8-ring" refers to a closed loop that

is built from 8 tetrahedrally coordinated silicon (or aluminum) atoms and 8 oxygen atoms. These rings are not always perfectly symmetrical due to a variety of effects, including strain induced by the bonding between units that are needed to produce the overall structure, or coordination of some of the oxygen atoms of the rings to cations within the structure. Therefore, the pores in many zeolites are not cylindrical.

Zeolite Type A

In the most common commercial zeolite, Type A the tetrahedron are grouped to form a truncate octahedron at each point. This structure is known as a sodalite cage. It contains a small cavity that is of no practical significance since the largest openings through the six-sided faces of the octahedron are not large enough to permit the entrance of even small molecules.

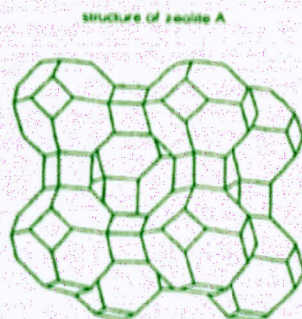


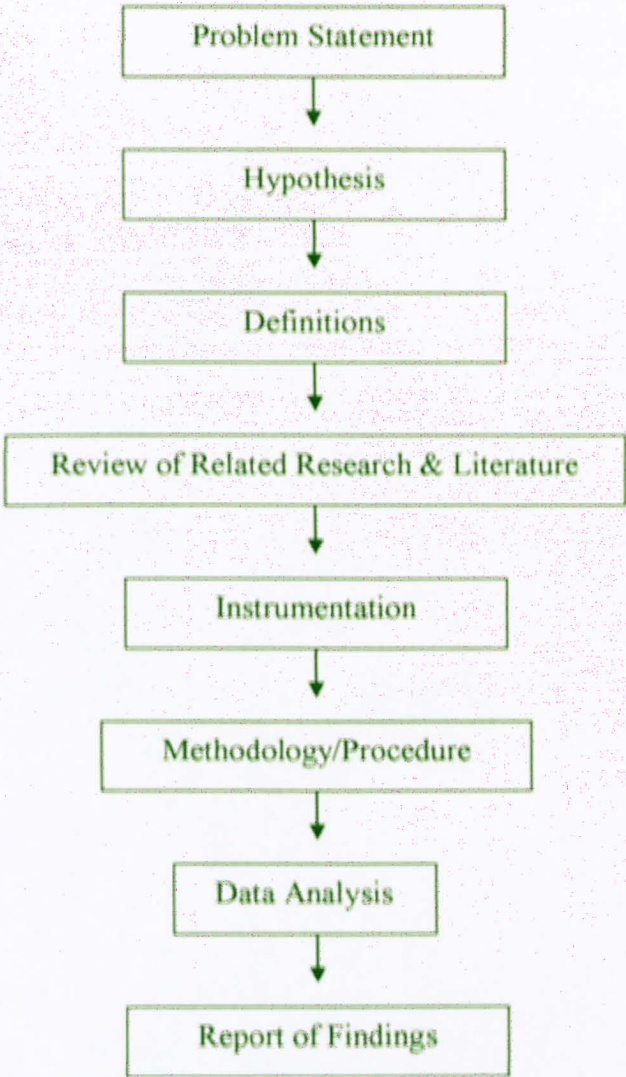
Figure 2.4: Structure of Zeolite A

When sodalite cages are stacked in simple cubic forms, the result is a network of cavities approximately 11.5Å in diameter, accessible through openings on all six sides. These openings are surrounded by eight oxygen ions. One or more exchangeable cations also partially block the face area. In the sodium form, this ring of oxygen ions provides an opening window of 4.2Å in diameter into the interior of the structure.

CHAPTER 3 METHODOLOGY

3.1 *Research Methodology*

The research methodology used is according to scientific research methodology.



3.2 Project Activities

Date	Project activities
27/7/2009	Consultation with Dr Lau
	- Revised previous progress.
	- Plan for next step in simulation.
31/7/2009	Calculation for parameters in equations used.
	- Calculate the parameters needed in the mass balance and source term.
7/8/2009	UDF Coding
	- Develop UDF coding for the adsorption case
	-Consult Dr Lau regarding the coding
13/8/2009	Weekly Consultation with Dr Lau
21/8/2009	Submission Of Progress Report 1
27/8/2009	Weekly Consultation with Dr Lau
3/9/2009	Weekly Consultation with Dr Lau
10/9/2009	Weekly Consultation with Dr Lau
	- Run the coding in Fluent Simulation
TBA	Summation of Interim Report
TBA	Oral Presentation with Examiner

STUDENT'S NAME : FARAH LIYANA BINTI SAHAFEA @ SHAFIE

STUDENT'S ID : 7314

SUPERVISOR: DIR LAU KOK KEONG

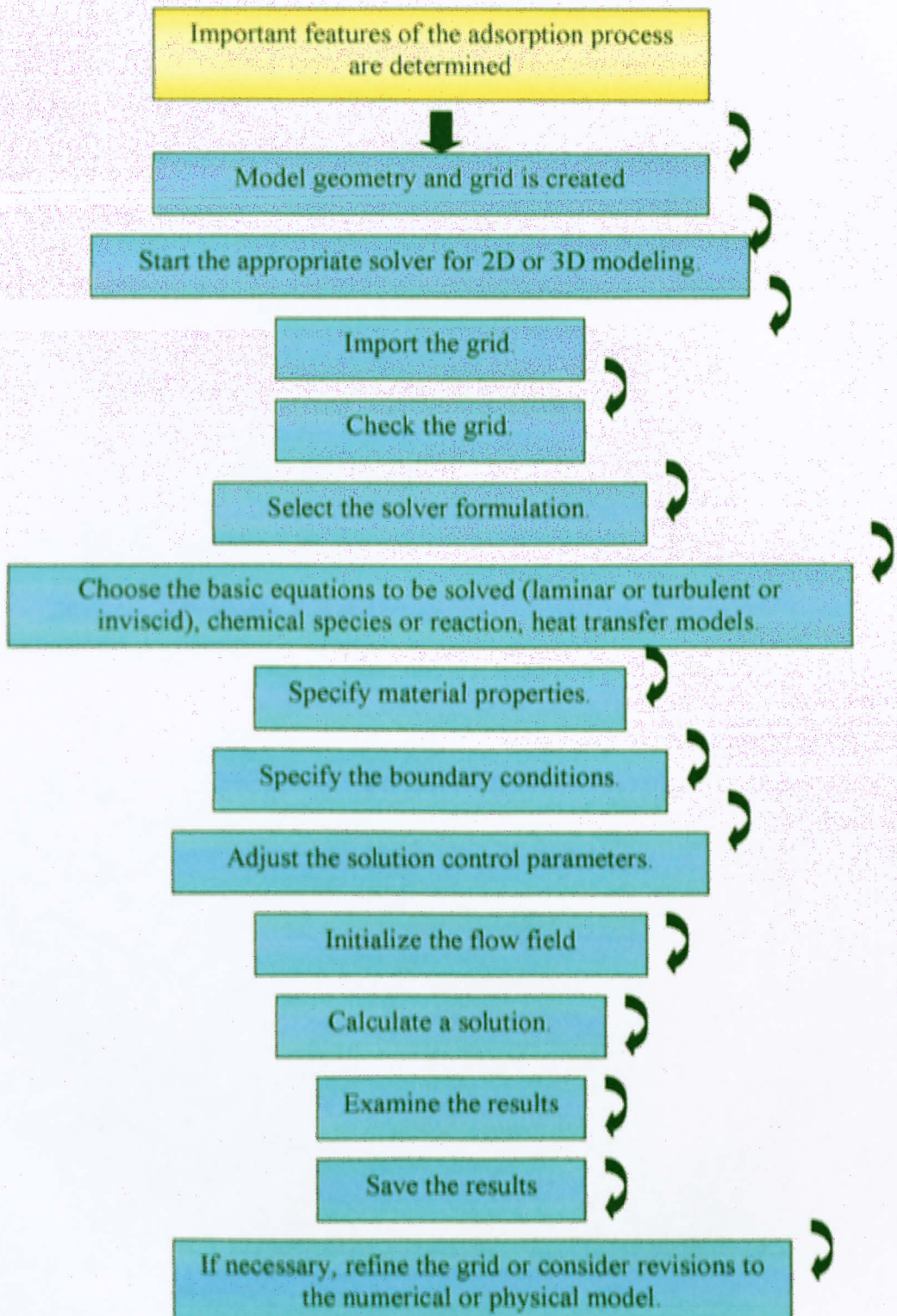
[illegible]

3.4 Tools/Software

ABOUT FLUENT

FLUENT uses unstructured meshes in order to reduce the amount of time you spend generating meshes, simplify the geometry modeling and mesh generation process, model more-complex geometries than can be handle with conventional, multi-block structured meshes, and let users adapt the mesh to resolve the flow field features. FLUENT can also use body fitted, block-structured meshes. FLUENT is capable of handling triangular and quadrilateral elements (or a combination of the two) in 2D, and tetrahedral, hexahedral, pyramid, and wedge elements (or a combination of these) in 3D. This exhibility allows user to pick mesh topologies that are best suited for your particular application. users can adapt all types of meshes in FLUENT in order to resolve large gradients in the flow field, but must always generate the initial mesh (whatever the element types used) outside of the solver, using GAMBIT, T Grid, or one of the CAD systems for which mesh import filters exist.

The steps and procedure is focused on the flow of modeling and simulating. Below explain the steps in using FLUENT 6.3.



CHAPTER 4

RESULTS AND DISCUSSION

4.1 DATA GATHERING/DATA ANALYSIS

4.1.1 Feed to the PSA Column (Natural Gas Composition)

TABLE 4.1: Natural Gas Composition and Relevant Properties

Component	Mole %
Methane	95.2
Ethane	2.5
Propane	0.2
iso - Butane	0.03
normal - Butane	0.03
iso - Pentane	0.01
normal - Pentane	0.01
Hexanes plus	0.01
Nitrogen	1.3
Carbon Dioxide	0.7
Oxygen	0.02

Natural gas consist of the a few components mention in (**Table 4.1**) above but methane cover more than 90% from the whole composition. Little amount of ethane, propane, butane, and other components is considered as impurities and therefore, in this study, methane as the main component is selected as the only component to represent natural gas. Mixture of H_2O/CH_4 is used in the amount of 50-50.

In order to express the inlet concentrations of H₂O and CH₄ Ideal Gas Law is used:

$$C_{Ao} = \frac{P_{Ao}}{RT_o} = \frac{y_{Ao}P_o}{RT_o}$$

where:

C_{Ao} = entering concentration of A [mol/mol/m³]

y_{Ao} = entering mole fraction of A

P_o = total pressure [Pa]

T_o = temperature [K]

P_{Ao} = partial pressure of A [Pa]

R = ideal gas constant [= 8.314 Pa·m³/(mol·K)].

Thus, the inlet concentration of both H₂O and CH₄ is 20.32mol/m³.

4.1.2 Adsorbent Properties

In the simulation, Zeolite 3A is used as the adsorbent. Physical properties of zeolite 3A are shown in *Table 4.2*.

TABLE 4.2: Physical Properties of Zeolite 3A

Property	Value	Source
Porosity	71%	Laboratory Specification
Bulk Dry Density	640 kg/m ³	Laboratory Specification
Surface Area	40.6 m ² /g	Laboratory Specification
Average Pore Diameter	1.9 nm	Laboratory Specification
Radius of Pellet	0.001 m	Laboratory Specification

4.1.3 Column Dimensions and Operating Conditions

PSA column dimensions and processing conditions that will be used in simulation are shown in *Table 4.3*

TABLE 4.3: Column Dimensions and Operating Conditions

Property	Value	Source
Width of the column	0.075 m	Laboratory Specification
Height of the column	0.300 m	Laboratory Specification
Pressure (adsorption step)	1 atm	Laboratory Specification
Inlet velocity	0.02 m/s	Laboratory Specification
Operating temperature	300 K	Laboratory Specification

4.1.4 Geometry of the Column

The PSA column schematic representation is shown in *Figure 4.1*.

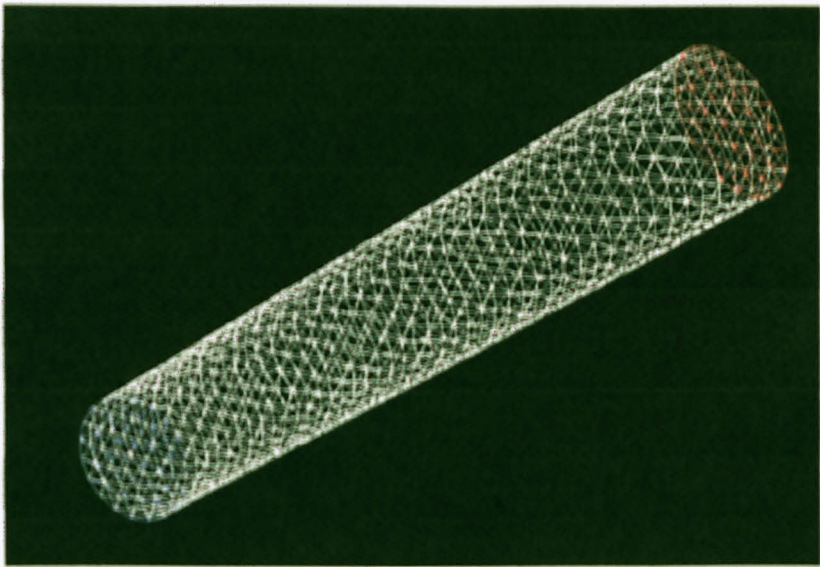


FIGURE 4.1: Geometry Obtained from GAMBIT Representing the Column

As shown in (*Figure 4.1*), the blue face at the bottom of the column represent inlet and red face at the top of the column represent the outlet. Side wall shown in white colour grid are insulated.

4.2 UDF CODE

The mass balance for the bulk flow in the bed or the interpellet phase is expressed by:-

$$-D_z \frac{\partial^2 C}{\partial z^2} + \frac{\partial uC}{\partial z} + \frac{\partial C}{\partial t} + \left(\frac{1-\varepsilon}{\varepsilon} ka(C - C_R^P) \right) = 0 \quad \leftarrow \text{Source term}$$

The term C_R^P which represent concentration at the pellet surface is replace with C^P because due to assumption that

$$(C - C_R^P) + (C_R^P - C^P) = (C - C^P)$$

$(C - C_R^P)$ = difference between concentration in bulk with concentration in interpellet surface

$(C_R^P - C^P)$ = difference between concentration in interpellet surface with concentration inside interpellet.

$(C - C^P)$ = difference between concentration in bulk with concentration inside interpellet.

In order to obtain the source term, Langmuir equation is used.

To simulate the adsorption within the column, Langmuir Equation is used in order to observe concentration decreasing along the packed bed column. Theoretically, for multicomponent gas, langmuir equation give:-

$$q = q_m^s(T) \frac{K_w(T)C_w}{1 + K_m(T)C_m + K_w(T)C_w}$$

(For nomenclature of each symbol, refer Nomenclature section)

So, in order to simulate this equation using FLUENT, UDF code is created:-

```
DEFINE_SOURCE(sourceH2O, c, t, dS, eqn)
{
    real CP;
    real s;
    real cmax=97.81;

    if (CP < C_UDSI(c,t,0))
    {
        CP=cmax*2.37*(C_UDSI(c,t,0))/(1+2.37*(C_UDSI(c,t,0))+0.16*(C_UDSI(c,t,1)));
        //CP=(cmax*36.365436*(C_UDSI(c,t,0)))/(1+(36.365436*(C_UDSI(c,t,0))+1.321926*(C_UDSI(c,t,1))));
        s = 0.000575243*pow((C_W(c,t)),0.33)*(C_UDSI(c,t,0)-CP); //recovery//
        //s = 0.000416635*pow((C_W(c,t)),0.6)*(C_UDSI(c,t,0)-CP); //uptake Curve//

        //printf ( "45a ", s);
    }
}
```

Figure 4.2: UDF code for uptake of water

```
DEFINE_SOURCE(sourceCH4, c, t, dS, eqn)
{
    real CP;
    real s;
    real cmax= 21.023;

    if (CP < C_UDSI(c,t,1))
    {
        CP=(cmax*0.16*(C_UDSI(c,t,1)))/(1+(2.37*(C_UDSI(c,t,0))+0.16*(C_UDSI(c,t,1))));
        //CP=(cmax*1.321926*(C_UDSI(c,t,1)))/(1+(36.365436*(C_UDSI(c,t,0))+1.321926*(C_UDSI(c,t,1))));
        s = 0.000575243*pow((C_W(c,t)),0.33)*(C_UDSI(c,t,1)-CP); //recovery//
        //s = 0.000329141*pow((C_W(c,t)),0.6)*(C_UDSI(c,t,1)-CP); //uptake Curve//

        //printf ( "46a ", s);
    }
}
```

Figure 4.3: UDF code for uptake of methane

4.3 PROPERTIES AND CONDITION FOR SIMULATION

4.2.1 Material Properties

As mention before, material used in the simulation is 50-50 mixture of methane and water. In FLUENT, the combination is defined in mixture species which H₂O/CH₄ is selected and properties of the mixture is generated automatically by the simulator as shown in **Figure 4.4**. These properties will be used throughout the simulation.

Mixture Species		names	((ch4 h2o) () ())
Density	kg/m3	incompressible-ideal-gas	#f
Cp (Specific Heat)	J/kg-K	mixing-law	#f
Thermal Conductivity	W/m-K	constant	0.045400001
Viscosity	kg/m-s	constant	1.72e-05
Mass Diffusivity	m2/s	constant-dilute-appx	(2.8799999e-05)
Thermal Expansion Coefficient	1/K	constant	0

Figure 4.4: Properties of H₂O/CH₄ generated by FLUENT

4.2.2 Boundary Condition and Solver

The solver used for the simulation is pressure based and in unsteady state condition as shown in **Figure 4.5** below.

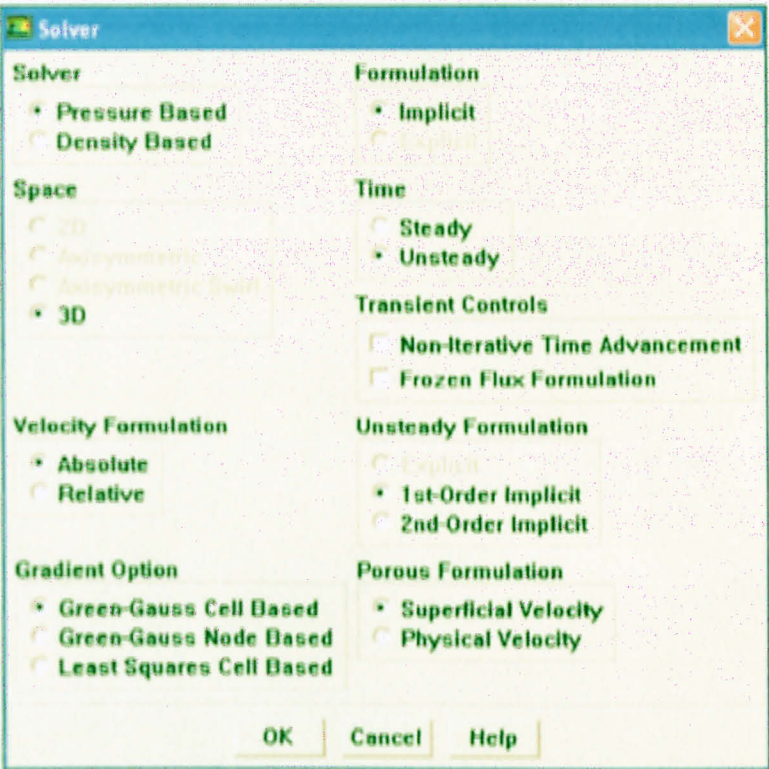


Figure 4.5: Solver

The overview of the adsorption can be demonstrated as in Figure 4.6 below:-

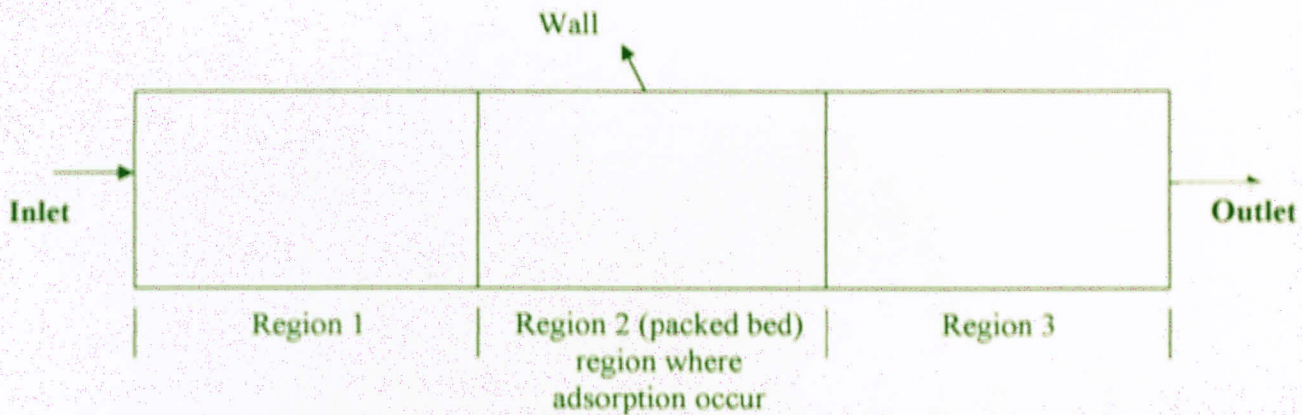


Figure 4.6: Overview of Adsorption Process

This figure shows how boundary condition is assign.

- Region 1: Fluid
- Region 2: Packed bed
- Region 3: Fluid
- Inlet: Velocity_inlet
- Outlet: Pressure_outlet
- Wall: wall

The velocity used for the simulation is 0.002m/s. the adsorption process will only occur along the packed bed region (Region 2) and this is the region where the UDF Code is interpreted.

4.4 RESULT GENERATED

Pressure

From the simulation, result of simulation is obtained as below:-

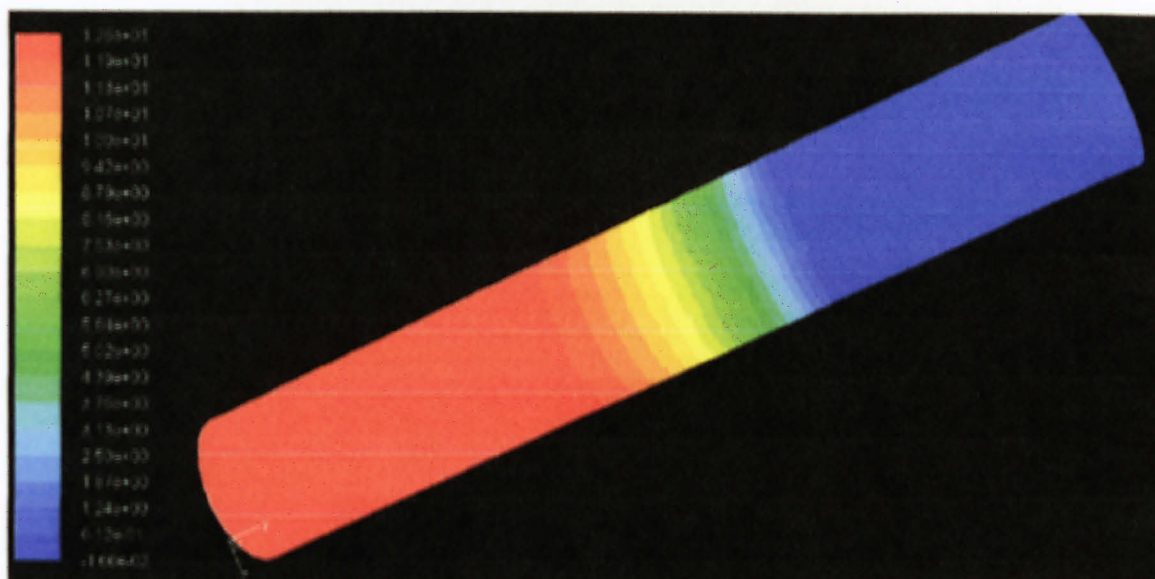


Figure 4.7: Pressure along Adsorption Column

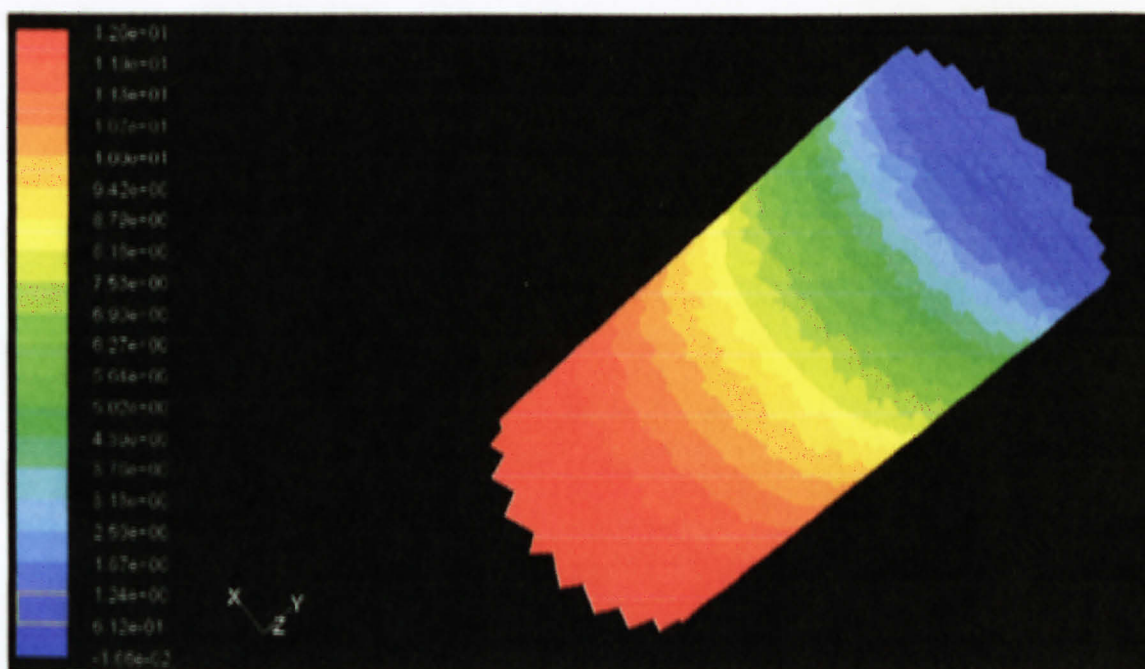


Figure 4.8: Pressure along Adsorption Column (Packed bed region only)

As shown in overview diagram above (**Figure 4.6**), the adsorption occurs in the packed bed (region 2) only which is at the middle region. **Figure 4.8** shows that along the packed bed, the pressure is decreasing until it reach minimum value. The red region is where the pressure is the highest while blue region indicates that the pressure is the lowest. The scale for pressure decreasing can be observed on the right of the figure. The pressure reduction shows that there are pressure drop across the bed from the inlet to the outlet.

The pressure drop along the column is quite small which 12.58 Pa. This pressure drop is the natural driving force in the adsorption bed. Different pressure between the inlet and outlet cause the natural gas to flow through the adsorption bed. Small value of pressure drop is quite good because it can increase the diffusional mass transfer resistance for adsorbing components of feed gas mixture into the adsorbent particle and create a mass transfer zone (MTZ) of significant size.

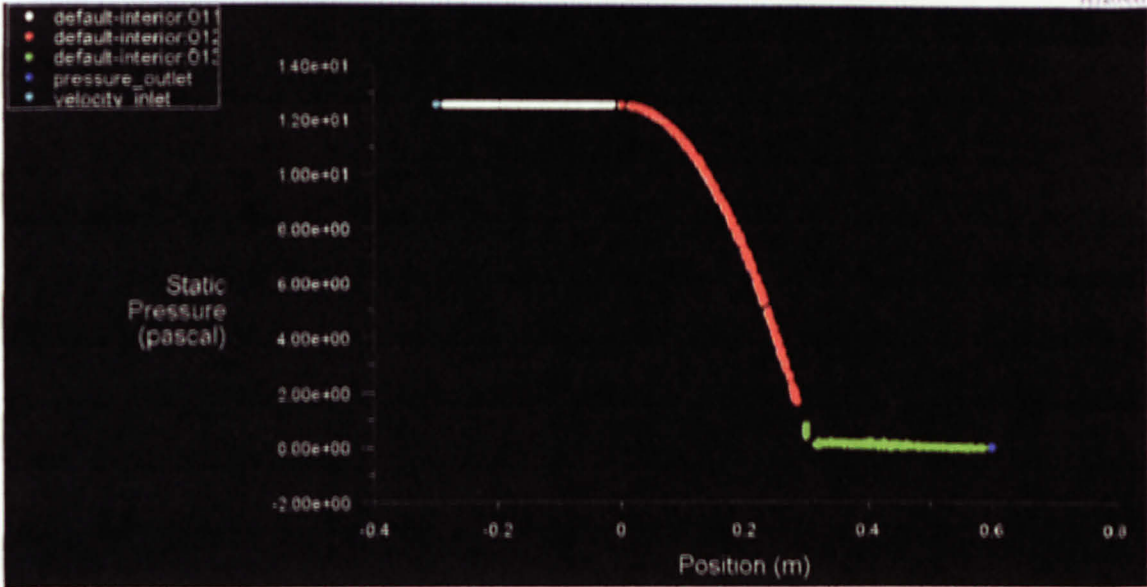


Figure 4.9: Position vs Pressure Curve

The graph in **Figure 4.9** showing pressure drop at the inlet until the outlet. The highest value of the pressure is 12.56Pa and the lowest pressure shown is -0.0166Pa. The total pressure drop along the adsorption bed is 12.58Pa.

To see effect of operating pressure in pressure drop, the simulation has been done in different operating pressure as indicate in table below:-

Flowrate (LPM)	Pressure (bar)	Pressure Drop
5	40	0.20666
	60	0.18302
	80	0.17077

Table 4.4: Pressure Drop

The result shows that increase in operating pressure result in lower in pressure drop. The importance to determine the pressure drop is to make sure that sufficient pressure can supplied by pump in order to cater the pressure loss. Low pressure drop is preferable for adsorption because high pressure drop will led to earlier breakthrough time. Low pressure drop also is favorable as it indicates that less energy loss within the column.

Graph of Operating Pressure vs Pressure Drop

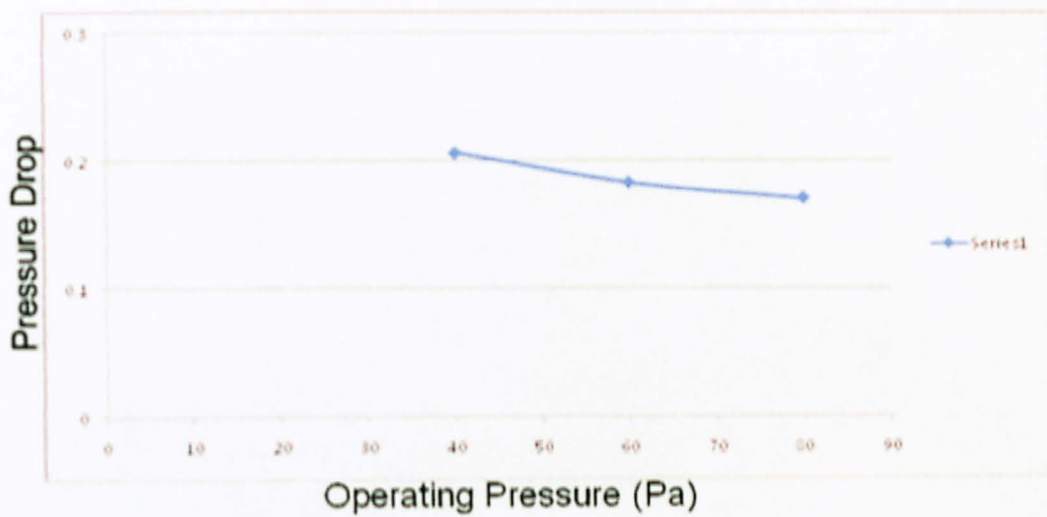


Figure 4.12 Graph of Operating Pressure vs Pressure Drop

Temperature

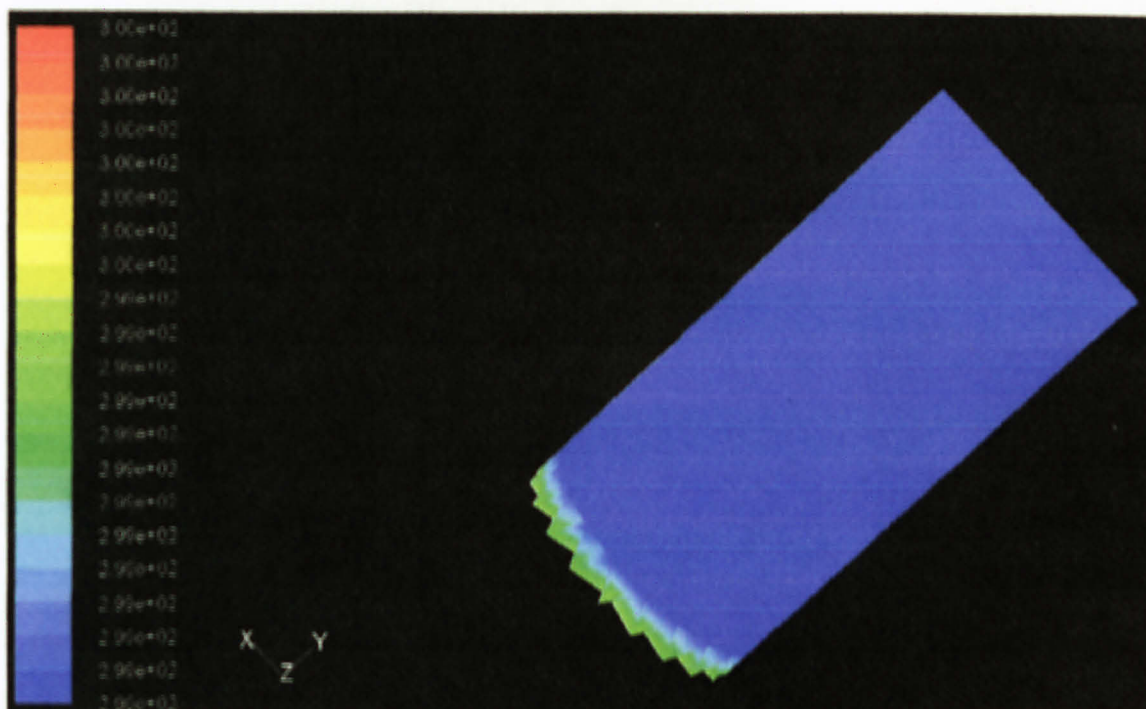


Figure 4.10: Temperature along Adsorption Column (packed bed)

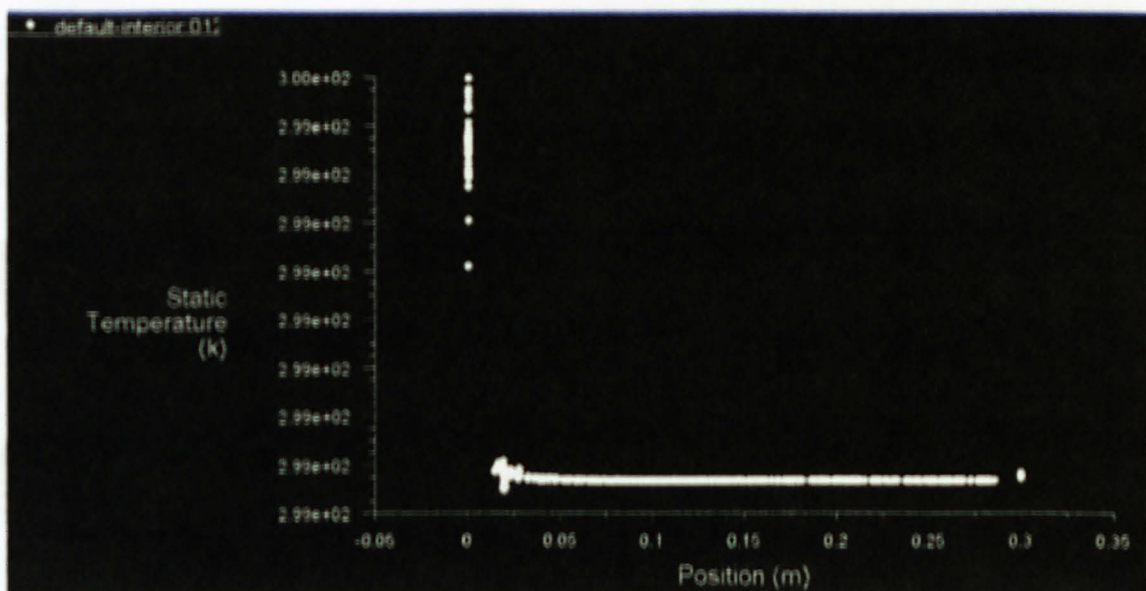


Figure 4.11: Position vs Temperature Curve

The temperature throughout the packed bed is 300K since the bed has already been set into that specific operating temperature. There is no variation in the temperature because only mass transfer is simulated in this simulation. There are no heat transfer occur along the packed bed. In the future, heat transfer must be included because all models for and adsorption bed must include:-

1. Adsorption isotherm
2. Mass and heat balance in interpellet gas phase
3. Mass and heat balance inside each pellet.

Since the main objective of this project is to see the efficiency of the bed in adsorbing H_2O from mixture of H_2O/CH_4 , only mass transfer is being given priority. So, variation of temperature is not observed in this project.

CHAPTER 5

CONCLUSION AND RECOMMENDATION

From the results obtained in this work several general conclusions can be drawn as follows:

- FLUENT 6.3 can be used to model quite complex processes such as adsorption step of the H_2O removal from natural gas.
- Model of adsorption process for H_2O removal from natural gas is able to give an insight into the internal working of the equipment.
- The pressure drop in the column shows that the adsorption process occurs in the column and low pressure drop (12 Pa) indicate that this column has high efficiency in adsorbing H_2O .
- When operating pressure increase, pressure drop start to decrease and this is preferable in industry since high pressure drop cause higher pump pressure and led to earlier breakthrough time.

5.1 Recommendation

5.1.1 Varies other Parameter

To observe the effect of other parameter such as temperature and flow rate on the pressure drop.

5.1.2 Geometry of the Column

The geometry of the column could be increase to see more significant result on pressure drop along the column.

REFERENCES

- [1] Christie John Geankoplis "Transport Process and Separation Process Principles," Pearson Education International, 4th Edition: 2003.
- [2] Ralph T. Yang, "Adsorbents: Fundamentals and Applications", A John Wiley & Sons, Inc., Publication, 2003
- [3] Motoyuki Suzuki, "Adsorption Engineering", ELSEVIER Science Publisher, 1941
- [4] Martin Boldiš, Karel Melzoch, Irena Kratochvilová, Milan Kocirik and Mojmir Rychtera, "Dewatering Of Ethanol Using Zeolites - Dynamics of Sorption,"
- [5] Khairul Sozana Nor Kamarudin, Hanapi Bin Mat, Halimatun Hamdan, Faculty Of Chemical And Resource Engineering, Universiti Teknologi Malaysia, "Zeolite As Natural Gas Adsorbents,"
- [6] N. A. Modine and M. E. Chandross, "Multiscale Modeling Of Small Molecules in Zeolite-4a,"
- [7] Ralph T. Yang, "Gas Separation By Adsorption Process" Imperial College Press, 1997
- [8] Internet Sources:
 - I. http://www.fs.utm.my/index.php?option=com_content&view=article&catid=56%3Aresearch&id=343%3Azeolite-and-nanostructured-material-group-znmg&Itemid=85, "Zeolite And Nanostructured Material Group"
 - II. <http://www.qbjohnson.com/?p=10365>, "TEG Dehydrator"
 - III. http://www.newpointgas.com/project_detail.php?id=161, "1 MMSCFD TEG Dehydrator & Two Stage Membrane Unit"
 - IV. <http://www.uniongas.com/aboutus/aboutng/composition.asp>, "UnionGas, A Spectra Energy Company."
 - V. <http://www.naturalgas.org/overview/background.asp>, "Natural Gas Organization"

APPENDIX I

Notations:

D_z = axial dispersion coefficient, $12.66 \text{ m}^2/\text{s}$

u = interstitial velocity, 0.000171 kg/m.s

C = interpellet concentration, mol/m^3

ε = interpellet void fraction, m

a = exterior surface area of pellets per volume of bed, m^2/m^3

k = average mass transfer film coefficient, dimensionless

C_R^p = concentration at the pellet surface, mol/m^3

t = time, s

z = distance in the bed from entrance, m

q = amount of water adsorbed on zeolite, mol/kg

q_m^z = maximum adsorption capacities for natural gas, mol/kg

K_w = constant, dimensionless

K_m = constant, dimensionless

C_w = concentration of water vapor, mol/m^3

C_m = concentration of natural gas, mol/m^3

M_m = Molecular weight of Methane, kg/kmol

M_w = Molecular weight of water, kg/kmol

σ_m = Constant in the Leonard-Jones potential-energy for methane, angstrom

σ_w = Constant in the Leonard-Jones potential-energy for water, angstrom

σ_{mw} = Constant in the Leonard-Jones potential-energy for the mixture, angstrom

ε_m = Characteristic Lennard-Jones energy for methane, dimensionless

ε_w = Characteristic Lennard-Jones energy for water, dimensionless

ε_{mw} = Characteristic Lennard-Jones energy for mixture, dimensionless

Ω_{mw} = Collision integral, dimensionless

R_p = radius of zeolite pellet, 0.002 m

μ =viscosity of mixture, Poise

ρ =density of mixture, 0.729kg/m^3

G =superficial mass flux, $\text{kg/m}^2.\text{s}$

k =average mass transfer film coefficient

k = Boltzman constant

Sh =Sherwood number

Sc = Schmidt number

Re =Reynolds number

APPENDIX II

The mass balance for the bulk flow in the bed or the interpellet phase is expressed by:-

$$-D_z \frac{\partial^2 C}{\partial z^2} + \frac{\partial uC}{\partial z} + \frac{\partial C}{\partial t} + \frac{1-\varepsilon}{\varepsilon} ka(C - C_R^P) = 0$$

The term C_R^P which represent concentration at the pellet surface is replace with C^P because due to assumption that

$$(C - C_R^P) + (C_R^P - C^P) = (C - C^P)$$

$(C - C_R^P)$ = difference between concentration in bulk with concentration in interpellet surface

$(C_R^P - C^P)$ = difference between concentration in interpellet surface with concentration inside interpellet.

$(C - C^P)$ = difference between concentration in bulk with concentration inside interpellet.

From Langmuir equation, the amount of water and natural gas adsorbed onto zeolite 3A can be expressed as

$$q = q_m^*(T) \frac{K_w(T)C_w}{1 + K_m(T)C_m + K_w(T)C_w}$$

q is in mol/kg but to fit the C^P term which is in mol/m³, q is multiplied with density.

This equation is to examine the selectivity of adsorption between water and natural gas onto the surface of zeolite.

To obtain average mass transfer film coefficient, k , Ranz Marshall equation is used:

$$\frac{2kR_p}{D_m} = 2.0 + 0.6 \left(\frac{\mu}{\rho D_m} \right)^{1/3} \left(\frac{2R_p G}{\mu} \right)^{1/2}$$

But first, to obtain molecular diffusivity D_m , Chapman-Enskog equation is used:-

$$D_m = 0.0018583 \frac{T^{3/2} (1/M_m + 1/M_w)^{1/2}}{P \sigma_{mw}^2 \Omega_{mw}}$$

$$\Omega_{mw} = \frac{A}{T^{*B}} + \frac{C}{\exp(DT^*)} + \frac{E}{\exp(FT^*)} + \frac{G}{\exp(HT^*)}$$

$$\sigma_{mw} = 3.1995 \text{ \AA}$$

$$\varepsilon_{mw} = 4.786 \times 10^{-21}$$

$$T^* = kT / \varepsilon_{mw} = 0.865$$

$$\begin{aligned} \Omega_{mw} &= \frac{A}{T^{*B}} + \frac{C}{\exp(DT^*)} + \frac{E}{\exp(FT^*)} + \frac{G}{\exp(HT^*)} \\ &= 1.085 + 0.1278 + 0.276 + 0.061 \\ &= 1.5498 \end{aligned}$$

So,

$$\begin{aligned} D_m &= 0.0018583 \frac{T^{3/2} (1/M_m + 1/M_w)^{1/2}}{P \sigma_{mw}^2 \Omega_{mw}} \\ &= 0.2089 \text{ cm}^2/\text{s} \\ &= 0.00002089 \text{ m}^2/\text{s} \end{aligned}$$

As mention above, mass transfer data in packed beds have been correlated by the Ranz-Marshall equation:-

$$\frac{2kR_p}{D_m} = 2.0 + 0.6 \left(\frac{\mu}{\rho D_m} \right)^{1/3} \left(\frac{2R_p G}{\mu} \right)^{1/2}$$

Or

$$Sh = 2.0 + 0.6 Sc^{1/3} Re^{1/2}$$

$$\begin{aligned} k &= \frac{2.0 + 0.6 \left(\frac{0.000171}{(0.729)(0.00002089)} \right)^{1/3} \left(\frac{2(0.002)(0.03645)}{0.000171} \right)^{1/2} \times (0.00002089)}{2 \times (0.002)} \\ &= 500.00 \end{aligned}$$

$$a = \frac{3}{R_p}$$

$$= 3/0.002$$

$$= 1500 \text{ m}^2 \text{ of pellet surface area/ m}^3 \text{ volume of bed}$$

$$\frac{\varepsilon D_z}{D_m} = 20 + 0.5 \text{Sc Re}$$

$$D_z = \frac{(20 + 0.5 \text{Sc Re}) D_m}{\varepsilon}$$

$$= \frac{[20 + 0.5(0.001123)(0.853)](0.00002089)}{0.33}$$

$$= 1.266 \times 10^{-3}$$

$$\Gamma = \rho D_z$$

$$= (0.729) \times (1.266 \times 10^{-3})$$

$$= 9.229 \times 10^{-4}$$

All calculation to obtain properties for mixture from individual properties of water and methane is shown below.

Calculation for properties of water and methane:

To calculate viscosity of mixture, μ , Wilke correlation is used:-

$$\phi_{mw} = \frac{[1 + (\mu_m / \mu_w)^{1/2} (M_w / M_m)^{1/4}]^2}{\{8[1 + (M_m / M_w)]\}^{1/2}}$$

$$\phi_{wm} = \phi_{mw} \frac{\mu_w M_m}{\mu_m M_w}$$

$$\mu = \frac{y_m \mu_m}{y_m + y_w \phi_{mw}} + \frac{y_w \mu_w}{y_w + y_m \phi_{wm}}$$

$$\mu_m = 0.00020$$

$$\mu_w = 0.00013$$

$$y_m, y_w = 0.5$$

From calculation:-

$$\phi_{mw} = 1.15$$

$$\phi_{wm} = 0.67$$

$$\begin{aligned} \mu &= \frac{0.5(0.00020)}{0.5 + 0.5(1.15)} + \frac{0.5(0.00013)}{0.5 + 0.5(0.67)} \\ &= 0.000171 \end{aligned}$$

Density of mixture calculation, ρ

$$\rho_m = 0.741 \text{ kg/m}^3$$

$$\rho_w = 0.717 \text{ kg/m}^3$$

$$\begin{aligned} \rho &= \rho \sum_{i=1}^n y_i \rho_i \\ &= 0.5(0.741) + 0.5(0.717) \\ &= 0.729 \text{ kg/m}^3 \end{aligned}$$

Superficial mass flux, G :-

Flowrate, ν is assume to be 0.05m/s

Mass flowrate, $M_f = \nu \times A \times \rho$

$$A = \pi r^2 = 0.0176\text{m}^2$$

$$\rho = 0.729\text{kg/m}^3$$

$$M_f = 0.05\text{m/s} \times 0.0176\text{m}^2 \times 0.729\text{kg/m}^3$$

$$G = M_f / A$$

$$= 0.03645\text{kg/m}^2.\text{s}$$

Leonard-Jones potential energy constant calculation:-

$$M_n = 16.043$$

$$M_w = 18.02$$

$$\sigma_n = 3.758\text{\AA}$$

$$\sigma_w = 2.641\text{\AA}$$

$$\sigma_{nw} = \frac{\sigma_n + \sigma_w}{2}$$

$$= \frac{3.758 + 2.641}{2}$$

$$= 3.1995\text{\AA}$$

Leonard-Jones potential energy constant calculation:-

$$\epsilon_n = 2.051 \times 10^{-21}$$

$$\epsilon_w = 1.117 \times 10^{-20}$$

$$\epsilon_{nw} = (\epsilon_n \epsilon_w)^{1/2}$$

$$= [(2.051 \times 10^{-21}) (1.117 \times 10^{-20})]^{1/2}$$

$$= 4.786 \times 10^{-21}$$